Paleovegetation dynamics in a montane vegetation mosaic in the Western Ghats, India: evidence for alternative stable states in the past?

Prabhakaran Ramya Bala[1], Sarath Pullyottum Kavil[2], Ichiro Tayasu[3], Chikage Yoshimizu[3], Kaustubh Thirumalai[4], Krishnan Sajeev[5], and Raman Sukumar[5]

[1]University of Pennsylvania
[2]Sorbonne University
[3]Research Institute for Humanity and Nature
[4]University of Arizona
[5]Indian Institute of Science

November 26, 2022

Abstract

Ecologists have proposed that montane grassland-shola (stunted evergreen forest) mosaics in the Western Ghats may represent alternative stable vegetation states. But paleoecology investigations seldom consider this framework, especially the role of short-term disturbances (fire, intense drought) other than long-term climatic changes, that can cause vegetation switches in landscapes with alternative vegetation states. The Sandynallah valley that hosts one of the oldest peat accumulations in the world at >50 kyr has been central to the reconstruction of paleovegetation in the montane Nilgiris, Western Ghats. Although the peat-forming vegetation here (dominated by sedges) is a unique vegetation state, its contribution to the paleovegetation signal has not been explicitly considered. We propose a conceptual framework of a tri-stability landscape with sedgeland on the valley floor, grassland on the hill slopes and shola vegetation in the boundary between sedgeland and grassland. While frost prevents shola saplings from establishing in grassland, waterlogging provides a barrier for their establishment in sedgeland, thus maintaining these distinct vegetation states under the same climate. We investigated the stable carbon isotope signatures of the cellulose fraction from two well-dated peat cores (Cores 1 and 2) collected from ˜170m apart in the Sandynallah valley within the alternative stable states framework. We find that Core 1, which is closer to the boundary of valley and hill slope, shows dynamic switches between sedgeland and shola whereas Core 2, located in the centre of the valley floor, represents a stable sedgeland state. The vegetation switches and maintenance mechanisms at Core 1 is connected to a disturbance (fire) and to changing climate while Core 2 seems to be responding primarily to climatic changes. The simultaneously distinctive vegetation states in Cores 1 and 2 at such close proximity within the same valley is the first record of alternative stables states in the past in the Western Ghats.

Paleovegetation dynamics in a montane vegetation mosaic in the Western Ghats, India: evidence for alternative stable states in the past?

Prabhakaran Ramya Bala[a,b,c,1], Sarath Pullyottum Kavil[a,2], Ichiro Tayasu[e], Chikage Yoshimizu[e], Kaustubh Thirumalai[d], Krishnan Sajeev[a], Raman Sukumar[b,c]

[a]Centre for Earth Sciences, Indian Institute of Science, Bengaluru - 560012, India
[b]Centre for Ecological Sciences, Indian Institute of Science, Bengaluru - 560012, India
[c]Divecha Centre for Climate Change, Indian Institute of Science, Bengaluru - 560012, India
[d]Department of Geosciences, University of Arizona, USA
[e]Research Institute for Humanity and Nature, Kyoto, Japan

Prabhakaran Ramya Bala – pramyabala@gmail.com (Corresponding author)
Sarath Pullyottum Kavil – sarathp39@gmail.com
Ichiro Tayasu – ichirotayasu@chikyu.ac.jp
Chikage Yoshimizu - chikage@chikyu.ac.jp
Kaustubh Thirumalai – kaustubh@arizona.edu
Krishnan Sajeev – sajeev@iisc.ac.in
Raman Sukumar – rsuku@iisc.ac.in

Keywords: Nilgiris, shola-grassland, carbon isotope, peat, Holocene, late Pleistocene

[1]Department of Anthropology, University of Pennsylvania, Philadelphia – 19104, USA
[2]LOCEAN, Sorbonne University, Paris, France

Highlights

- Three stable vegetation states – grassland, shola, sedgeland - exist in montane Nilgiris
- Fires and intense droughts can cause vegetation switches in the ecotones
- Vegetation in the core sedgeland is primarily controlled by climatic change
- Shola retreated from grassland, expanded into sedgeland during the last glacial
- Simultaneously different vegetation represents alternative stable states in the past

Abstract

Ecologists have proposed that montane grassland-*shola* (stunted evergreen forest) mosaics in the Western Ghats may represent alternative stable vegetation states. But paleoecology investigations seldom consider this framework, especially the role of short-term disturbances (fire, intense drought) other than long-term climatic changes, that can cause vegetation switches in landscapes with alternative vegetation states. The Sandynallah valley that hosts one of the oldest peat accumulations in the world at >50 kyr has been central to the reconstruction of paleovegetation in the montane Nilgiris, Western Ghats. Although the peat-forming vegetation here (dominated by sedges) is a unique vegetation state, its contribution to the paleovegetation signal has not been explicitly considered. We propose a conceptual framework of a tri-stability landscape with sedgeland on the valley floor, grassland on the hill slopes and shola vegetation in the boundary between sedgeland and grassland. While frost prevents shola saplings from establishing in grassland, waterlogging provides a barrier for their establishment in sedgeland, thus maintaining these distinct vegetation states under the same climate.

We investigated the stable carbon isotope signatures of the cellulose fraction from two well-dated peat cores (Cores 1 and 2) collected from ~170m apart in the Sandynallah valley within the alternative stable states framework. We find that Core 1, which is closer to the boundary of valley and hill slope, shows dynamic switches between sedgeland and shola whereas Core 2, located in the centre of the valley floor, represents a stable sedgeland state. The vegetation switches and maintenance mechanisms at Core 1 is connected to a disturbance (fire) and to changing climate while Core 2 seems to be responding primarily to climatic changes. The simultaneously distinctive vegetation states in Cores 1 and 2 at such close proximity within the same valley is the first record of alternative stables states in the past in the Western Ghats.

1. Introduction

The existence of forest and 'nonforest' mosaics in close proximity with abrupt transitions has been debated by ecologists for over a century (Pausas and Bond 2020). It is now widely accepted that vegetation mosaics represent stable vegetation states whose dynamics can be explained under the Alternative Stable States framework (Hirota et al. 2011; Hoffmann et al. 2012; Pausas and Bond 2020). Such vegetation mosaics in mountainous regions are seen in Malawi and Madagascar (Bond et al. 2008), the Patanas in Sri Lanka (Pemadasa and Amarasinghe 1982), the South Brazilian Campos (Overbeck et al. 2007), the grassy balds in the Bunya mountains of Australia (Moravek et al. 2013), South Appalachia in North America (Delcourt and Delcourt 1997) and the *shola* forest-grassland mosaics of the Western Ghats in India (Ranganathan 1938, Meher-Homji 1967). Traditionally, the global distribution of vegetation has been explained by climate, but the existence of strikingly different vegetation types (forest and grassland) in the same environment shows that climate cannot fully explain global vegetation (Bond 2005). In several of these biomes with montane forest-grassland mosaics, anthropogenic clearance of forests was considered to be a reason for grassland occurrence since grassland was believed to be an alien element in a climate suitable for the growth of forest vegetation; a tenet which dynamic global vegetation models support (e.g. Chaturvedi et al. 2011). It was believed that these anthropogenically degraded forests (montane grasslands), given enough time and protection from disturbances, would recover to a closed forest state (e.g. Pemadasa 1990). But these expectations run contrary to various paleoecological studies that point to the antiquity and abundance of montane grasslands in several of these mosaics much before the arrival and settlement of humans (Vasanthy 1988; Meadows and Linder 1993; Sukumar et al. 1993; Rajagopalan et al. 1997; Sutra et al. 1997; Behling and Pillar 2007; Moravek et al. 2013). This has led to the acceptance of the alternative stable vegetation states framework to explain montane grassland-forest mosaics (Joshi et al. 2020).

According to the alternative stable states theory, one climatic regime can support two or more stable vegetation states such that each state shows resilience by returning to its original state after small disturbances due to stabilizing feedback mechanisms (Pausas and Bond 2020). But a strong stochastic perturbation to the system or gradual shifts in environmental drivers can cause one stable state to move to an alternative state. The alternative state is also stable, stabilized through feedback mechanisms, while intermediate states are unstable. But the system may not revert to its original stable state even if the driver causing the perturbation is removed, due to hysteresis. When adapted to describe vegetation dynamics, the stable states apply to vegetation states whereas the perturbations to the system are stochastic disturbances (e.g. fires), or gradual changes in environmental drivers (e.g. temperature). Not all processes facilitating a vegetation switch can be reversed, so a switchback does not happen even when the disturbance causing the switch is reversed - this characteristic is called hysteresis.

An important characteristic of the alternative stable states framework in vegetation states is to establish a potential disturbance/ perturbation that pushes the system away from one stable state to either an intermediate unstable state or to the alternative stable state. The second characteristic is to establish maintenance pathways that provide a positive feedback to make

the state resilient despite the presence of small perturbations. The third characteristic is to establish stability, that these systems can survive longer than one generation. Maintenance mechanisms such as herbivory, periodic fires, precipitation changes have been proposed globally (Pausas and Bond 2020).

The tropical grassland-*shola* ('shola' is a word of Tamil origin for stunted evergreen forest patches) mosaic is characteristic of the montane region (>1800m asl), especially the Nilgiri and Anamalai hill ranges, of the Western Ghats (India) (Ranganathan 1938; Meher-Homji 1967). In the shola-grassland mosaics, frost occurring in the grasslands were observed to act as a barrier for trees (Ranganathan 1938, Meher-Homji 1967). Fires and mammalian herbivory (Bor 1938) and potential differences in soil nutrients were also proposed as barriers to tree establishment (Ranganathan 1938). Joshi et al. (2020) test soil and microclimate as drivers and propose that the shola-grassland represent alternative stable states with frost as the primary mechanism determining their spatial distribution. But establishing the stability of a vegetation state with long-lived species such as trees is difficult in practical terms (Bowman and Perry 2017). Paleoecology can provide historical information on disturbance regimes such as fires and help establish whether gradual changes in environmental drivers such as temperature would have direct impacts on the establishment and subsequent maintenance of alternate vegetation states.

One way to visualize alternative stable states would be to see strikingly different vegetation under the same climatic regime with sharp spatial boundaries. But how would such sharp spatial gradients vary temporally? Intuitively we can think of a mean vegetation state with small disturbances, shifting to a different mean state, is one way to demonstrate alternative stable states in the past. In Tasmania, where fire-mediated vegetation dynamics have been documented for over a century, four alternative stable states at the landscape level have been described: rainforest, eucalypt forest, sclerophyll shrubs and moorland (Murphy and Bowman 2012). Fletcher et al. (2014) propose a candidate profile which would fit the alternative stable states framework where palynological evidence for a shift in vegetation mean state from forested Cyperaceae-Sphagnum dominated sedgeland (and eucalypt forests) to non-forested Restionaceae (rush)-dominated wetland was observed after a catastrophic fire 7000 yrs ago. The new stable vegetation state gets maintained by a positive feedback mechanism: rhizomatous vegetation increases waterlogging, thereby preventing forest elements from establishing themselves. Another way of establishing alternative stable states would be to look at multiple profiles from adjoining sites (hence subject to the same climate, potential vegetation mosaics) and compare the paleovegetation, to find simultaneous existence of different vegetation states.

Although archives that preserve past vegetation to allow for paleoecological investigations in tropical southern India are scarce due to high levels of decomposition, the high altitude (>1800 masl) and cool temperatures (annual average 13.5˚C, mean maximum 18.5˚C, mean minimum 8.5˚C (von Lengerke 1977)) typically occupied by the shola-grasslands have facilitated multiple studies of paleovegetation and paleoclimate (Vasanthy 1988; Sukumar et al. 1993; Rajagopalan et al. 1997; Sutra et al. 1997; Caner et al. 2007; Raja et al. 2019). Prominent among the various archives used in these investigations is the Sandynallah valley with one of

the oldest peat accumulations in the world >50 kyr (Ramya Bala et al. 2016), that preserves Late Quaternary vegetation and climate (Vasanthy 1988; Rajagopalan et al. 1997; Sutra et al. 1997). These studies have broadly demonstrated the response of the vegetation to well-known global climatic events such as the Last Glacial Maximum, the Holocene Optimum and an additional phase of relatively arid and fluctuating monsoon (about 6–2 ka). Recently this valley has also been reported to preserve signatures of paleofires and human presence in this montane region at c. 3.5 ka (Kavil et al. 2020). Accordingly, Caner et al. (2007) state that *"The Nilgiri highlands have long been an oasis for paleoenvironmental research within an otherwise unrewarding South Indian craton in terms of Quaternary environmental archives"*.

One of the main historical debates to which paleoecology in the region has lent its use is on the origin of the grasslands in the region: are they anthropogenic or natural? Palynological studies from this site (Vasanthy 1988; Sutra et al. 1997; Suryaprakash 1999) show that the mosaic is indeed not anthropogenic in origin as evidenced by the abundance of grass pollen throughout the Holocene, extending into the last glacial (~35 ka). Sutra et al. (1997) found that *Graminae* and *Cyperaceae* together constitute the most abundant taxa (>60% throughout the profile) with *Graminae* constituting as much as 78% of total pollen counts in some parts of the deeper section, which were dated to circa 30 ka. They conclude that this vegetation mosaic indeed represents an apparent equilibrium of two natural climatic climaxes; with the grasslands representing the climatic climax of the frost zone, and the stunted evergreen forests: the forest zone (Vasanthy 1988).

Paleoecological investigations have utilized stable carbon isotopic differences in photosynthetic pathways – the C3 shola vegetation and predominantly C4 nature of grasslands (both C3 and C4 grasses exist here) -- to trace relative changes in biomass contribution from these two vegetation states and by extension, changing climate. This is based on the principle that the stable carbon isotope composition (measured by $\delta^{13}C$) of global vegetation shows a bimodal distribution with significantly different values between the C4 and C3 photosynthetic pathways (O'Leary 1988). Average values reported by Basu et al. (2015) for a tropical plant database from eastern India is -12.7 ± 1.4‰ and -29.6 ± 1.9‰ respectively. The differences in photosynthetic pathways confer a physiological advantage to C4 plants at times of higher temperatures, lower water availability, and low atmospheric CO_2 (Ehleringer 1978). In the Nilgiris, a relatively less negative $\delta^{13}C$ value has been interpreted to represent the expansion of grasslands in glacial times, as opposed to a relatively greater C3 biomass contribution in the interglacial period, representative of shola expansion (Sukumar et al. 1993; Rajagopalan et al. 1997; Caner et al. 2007). This is also supported by the experimental work of Joshi et al (2020) that frost is the primary barrier to establishment of shola saplings in grasslands.

Thus far, no study has investigated the paleoecology of the montane Western Ghats within the alternative stable states framework. Within such a landscape, changes in spatially-heterogenous mean vegetation states arise even within a single climate regime due to disturbances such as fire or sustained drought. The small-scale and sharp boundaries across these vegetation states warrants a careful analysis of results from multiple peat cores at a temporal resolution fine enough to capture state changes. It is also important to point out that several authors have studied peatlands in this landscape as an archive of regional changes in the shola-grassland

mosaic. The vegetation of the peatlands here is unique to the valley floor, comprising of sedges, grasses, herbs and mosses. In order to differentiate the vegetation states clearly, we refer to this distinctive peat-forming vegetation as *sedgeland* (since sedges are not found in the grassland or shola) in this paper. We believe that it is pertinent to include the sedgeland as a potentially third stable vegetation state in this dual stability grassland-shola landscape to understand (paleo)vegetation dynamics in the montane Nilgiris more comprehensively, especially given the effects of climate on these states. In this work, our objective was to reconstruct sedgeland-shola-grassland vegetation dynamics at sufficiently high (~multicentennial-to-millennial-scale) temporal resolution, using stable carbon isotopes from two peat cores in the Sandynallah valley, and examine the evidence for alternative stable states.

2. Methods

2.1 Site details

Our study site, the Sandynallah valley, is located between 11°26'32"N 76°38'6"E and 11°26'37"N 76°38'8"E (Figure 1) at an elevation of ~2200 m asl., in the southern Western Ghats, India. This site receives annual average precipitation of about 1240 mm of which ~50% is from the South West and ~30% from the North East monsoon (von Lengerke 1977). The valley is underlain by charnockite of age ~2527±14 Ma (Samuel et al. 2014). The natural vegetation at Sandynallah is of grassland on the gentle slopes and rounded crests, *shola* vegetation (stunted evergreen forests) along some folds of the hills and in the toe slope, with distinctive peat-forming wetland vegetation in the valley floor.

a. The shola vegetation is typically composed of members of the *Lauraceae, Rubiaceae, Symplocaceae, Myrtaceae* and *Euphorbiaceae* (Sukumar et al. 1995). The trees that we observed in the fragmented shola patch near the sampling site are *Lasianthus venulosus, Turpinia nepatensis, Rubus elipticus, Withania somnifera, Michelia nilagirica, Buxus sp., Olea sp., Syzigium densiflorum, Rapanea wightii, Mahonia leschenaultii, Rhododendron nilagiricum, Symplocos obtusa, Elaeagnus conferta, Ligustrum roxburghii* and the invasive species *Acacia mearnsii*.
b. The grasslands in the montane Nilgiris are reported to have dominant grass species *Andropogon lividus Thw., Arundinella vaginata Bor, Digitaria wallichiana Stapf., Arundinella mesophylla Nees. ex Steud* (Jose et al. 1994). The grassland at Sandynallah also supports ferns, *Pteridium sp.*, herbs of *Asteraceae, Auxalidaceae* and *Begoniaceae*, the carnivorous *Drosera sp.* as well as the invasive *Ulex europaeus*.
c. The wetland in the valley floor (referred to as 'sedgeland' in this paper) is dominated by *Cyperaceae (Fimbristylis spp., Cyperus spp.)* and *Poaceae (e.g. Eragrosus sp.)*, several herbaceous members of *Scrophulariaceae, Asteraceae, Polygonaceae, Eriocaulaceae, Gentianaceae* and a few mosses of *Polytrichidae*.

Caner et al. (2007) point out that the Sandynallah valley, due to its location in the central Nilgiris in an intermediate precipitation and wind strength zone, would be especially sensitive to small changes in temperature and precipitation as opposed to the western Nilgiris. This behaviour is typical of ecotones, whereby climatic changes are preserved more sharply near a

vegetation boundary than in the ecological core zone where greater amplitudes of climatic change are necessary to result in vegetation changes. Two sites were chosen for coring from a relatively less disturbed broad valley at Sandynallah. The first site was closer to the edge of the hill surrounding the valley and the second site was ~170m along the length of the valley from the first site and possibly less disturbed than the earlier site (Figure 1). The valley is part of the Sheep Breeding Research Station (SBRS), maintained by the Tamil Nadu Agriculture and Veterinary Sciences University (TANUVAS), from whom permissions were obtained to carry out this work.

Figure 1: a) Coring locations in the main valley at Sandynallah showing grasslands on the ridges and gentle slopes, sedgeland in the valley floor and a large patch of woody shola vegetation (top right), woody stems are also seen close to Core 1 location, b) A view from the head of the valley, facing North-East

2.2 Resistivity Survey

A resistivity survey of the site was first undertaken to inform us about sub-surface structures that might create impediments for manual coring. The survey was conducted by the Elite Engineering Consultancy. The details from the report provided by the company is reproduced here. Four electrodes were driven into the earth along straight line at equal intervals. A current *I* was passed through the two outer electrodes and the earth and the voltage difference *V*, observed between the two inner electrodes. The current flowing into the earth produces an electric field proportional to its density and to the resistance of the soil. The voltage measured between the inner electrodes is, therefore, proportional to the field. Consequently, the resistivity will be proportional to the ratio of the voltage to current. Resistivity was then calculated based on the formula, $\rho = 2\pi.a.R$, where, a = Distance between two consecutive electrodes, R = Observed resistance. The survey was conducted in the main Sandynallah valley (>40 kyr old) locations 1 & 2, at distances of 0.5, 1, 1.5, 2, 5, 7.5 and 10 m distances in all 4 directions (Figure 2).

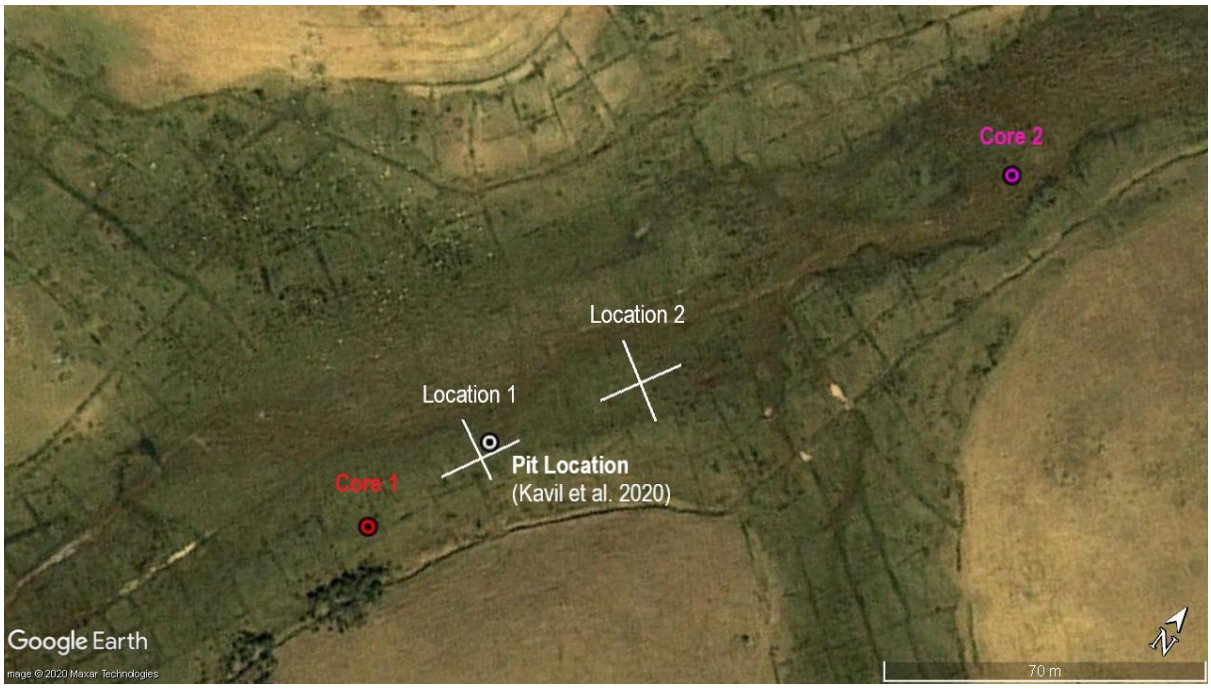

Figure 2: Locations 1 and 2 where resistivity survey was conducted, locations of the pit for excavation samples reported in Kavil et al. (2020), Cores 1 and 2 (this study)

2.3 Coring and sub-sampling

For achieving a fine temporal resolution in an undisturbed core, peat sampling was carried out using a Belarussian Peat corer (Jowsey 1966). This is a D-type corer, 5 cm in width and 50 cm in length. The corer is manually operated and has two extension rods which were graduated at the time of coring for sub-surface depths and peat sampled from the Sandynallah valley during the dry season in the months of January - February 2012 using a predefined sampling strategy (De Vleeschouwer et al. 2010). Each master core comprises of 9 core units, with 10 cm overlap between successive core units at either ends, procured from bore holes ~30 cm apart to account

for lateral variation and to ensure non-disturbance from the coring head (see Figure 3 for sampling design). Two master cores were obtained from 2 pairs of boreholes ~170 m apart, spanning a depth of 3.7m (these cores will hereafter be referred to as Cores 1 and 2). The cores were preserved in a -20˚C freezer near the sampling site after collection until further use to avoid disintegration during transportation. A band saw with a stainless steel (SS) blade of 1 mm thickness was used to slice the frozen cores at ~1 cm (Core 1) and ~2cm (Core 2) each (Givelet et al. 2004). Precautions were taken to avoid contamination during these procedures. Gloves were washed between different core sections. The blade was washed well and rinsed with distilled water before proceeding to the next core section. If found soiled even after multiple washes, the band saw was opened, and all parts were cleaned meticulously before proceeding to next subsampling. The slices were placed into labelled sample containers and stored at -20˚C.

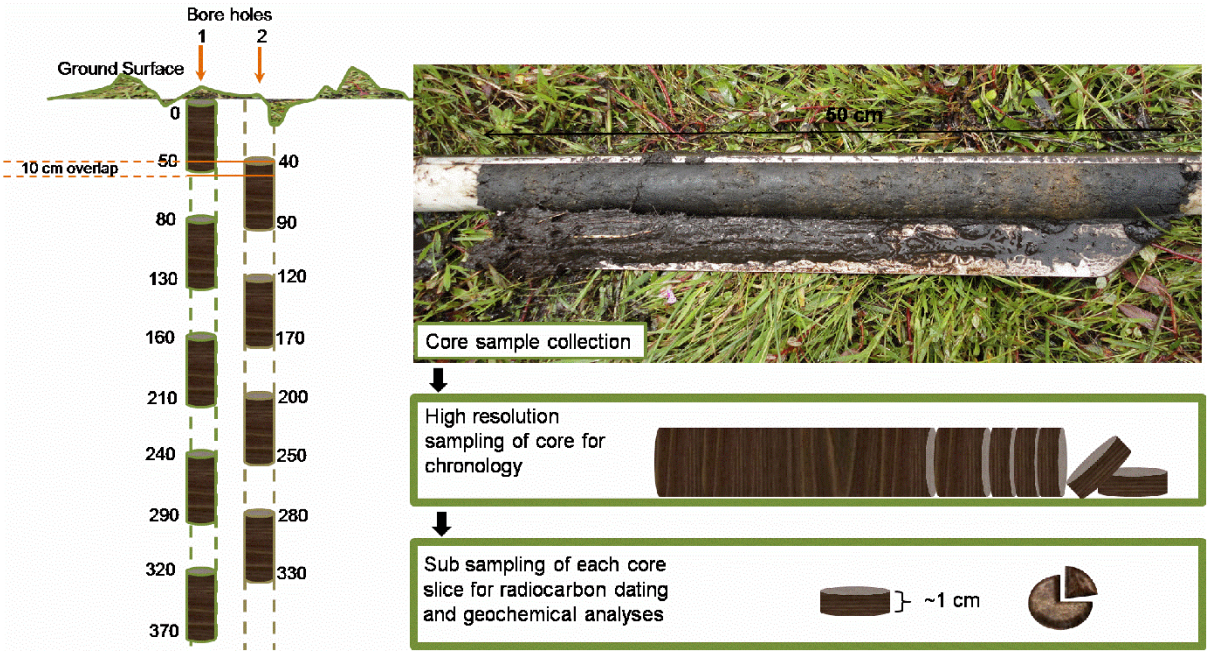

Figure 3.Sampling and sub-sampling strategy (reproduced with permission (Ramya Bala et al. 2016))

2.4 Chronology

2.4.1 Radiocarbon dating

About 2 to 3 g of wet samples (Core 1 – 73, Core 2 – 40) were used directly for radiocarbon measurements. The standard Acid-Alkali-Acid pre-treatment method was used for chemical extraction of the desired carbon fraction followed by combustion, CO_2 purification and graphitization (Nakamura et al. 2003). The ^{14}C measurements were performed on a Tandetron accelerator mass spectrometer (Model-4130 AMS, HVEE), at the Division for Chronological Research, Nagoya University. We used the HOx-II standard (NIST new oxalic acid standard, SRM-4990C) as a reference of carbon isotope ratios and commercial oxalic acid containing no ^{14}C (oxalic acid dihydrates, prod. No. 57952, produced from Wako Pure Chemical Industries Ltd., Japan) for ^{14}C blank subtraction in the data analysis. We repeated three to five runs of ^{14}C measurements on a group of samples loaded at one time in the ion source of AMS system. We

calculated ^{14}C content of the sample in each run, and an average value and an error were obtained for the results from several runs. This error value is reported as the *internal error*. We also experimented with pre-treatment protocols to arrive at a *laboratory error* for our radiocarbon ages. The details of the high-resolution chronology have been described elsewhere (Ramya Bala et al. 2016).

2.4.2 Age-Depth Modelling

For the radiocarbon ages obtained from the AMS laboratory, we calculated a modified error which accounts for both *internal error* and estimated *laboratory error* (described in detail in Ramya Bala et al. (2016)) following the method recommended in Calib (Stuiver and Reimer 1993). We modelled the age-depth relationship using a published Bayesian age-depth modelling software *Bacon v2.2* (Blaauw and Christen 2011). In tropical peat, inversions are common in the radiocarbon profile, possibly due to deep-rooted vegetation (Ramya Bala et al. 2016). But the Bayesian model does not account for reversals in the profile and hence we restricted our analyses to the section of the profile where major inversions do not occur. In the case of Core 1, the 10 cm overlap between core units was also dated to get an estimate of lateral variation in the substratum. Since the lateral variation in dates was significant, modelling the units as one profile caused the model to reject the lateral variations as inversions. Hence core units in Core 1 were modelled individually to assign dates for the proxy results while in Core 2 we modelled the entire core as one profile since information on the overlap sections was not available.

2.5 Stable Isotope analysis

2.5.1 Cellulose Extraction

The core slices were freeze-dried and homogenized by hand using mortar and pestle. About 1 gm of the powdered bulk peat was used for cellulose extraction following the principles used in the paper pulp manufacture process. This method was first used by Brenninkmeijer et al. (1982), and subsequently adapted by Rajagopalan (1996). The bulk peat was first treated with distilled water to remove soluble impurities, then treated with acid to remove carbonates and acid-soluble organics. Following neutralization, samples were treated with alkali for a long duration to remove the humic fraction. This was followed by acidified sodium chlorite treatment for delignification: several rounds of addition over 8 hours under constant heat (~60 ºC) on a hotplate. The final solution was sieved (63 µm mesh) and the fibres accumulating on the mesh collected. The fibre-rich water was then boiled with alkali to remove hemi-cellulose from alpha-cellulose. The fibres were then washed with excess water and stored at -20°C. The frozen cellulose in water was subsequently freeze-dried to yield fibres for analysis.

2.5.2 Isotope Ratio Mass Spectrometry

Carbon isotope ratios were measured on cellulose fractions for Cores 1 and 2 on an isotope ratio mass spectrometer (Delta V advantage, Thermo Fisher Scientific, Inc.) connected to an elemental analyser (Flash EA1112, Thermo Fisher Scientific, Inc.) via an interface (Conflo IV, Thermo Fisher Scientific, Inc.) at the Research Institute for Humanity and Nature, Kyoto,

Japan. Data were corrected by two internal standards, CERKU 03 (glycine, $\delta^{13}C$ = -34.92‰) and CERKU 07 (corn starch, $\delta^{13}C$ = -10.76‰) which were calibrated with multiple international standards (Tayasu et al. 2011). A routine precision of the internal standards was < ±0.1‰. We analysed 174 unique cellulose extracts and 5 triplicates, 6 duplicates to estimate sample heterogeneity (cellulose is fibrous, hence there is the risk that a bunch of fibres pulled for analysis might be representative of one plant tissue). We found an average standard deviation of 1.06‰ among triplicates (maximum 2.91‰, minimum 0.15‰).

2.6 Disturbance records

We use the information recorded in excavation samples from a pit in the Sandynallah valley close to Core 1 (Figure 2) reported by Kavil et al. (2020). Fires are reported at ~22 ka (macrocharcoal) and ~3.5 ka (macro-, microcharcoal and charcoal/pollen ratio). They also report peat surface wetness using alkane biomarker derived proxy P_{aq}, defined as C23+C25/C23+C25+C27+C29. It is the proportion of hydrocarbons from submerged and/or floating aquatic macrophytes relative to the input from terrigenous and immersed plants. Higher P_{aq} value is an indicator of surface wetness in the peatland which can also be inferred as increased precipitation.

3. Results

3.1 Resistivity Survey

Up to a depth of 2 m, the peat substratum shows a higher resistance per unit depth (Figure 4). From 2 – 10 m, in all directions (except location 1 - East) the medium is homogenous and continuous in stratigraphy without any sudden jumps in values. The peats are homogeneous both vertically and laterally as is seen from the plots. The profiles generated were found to be reliable as illustrated by the sudden resistivity increase in Location 1 - East, which was taken very close to the toe slope, possibly because of an underlying basement. Due to the slightly higher elevation in that direction, the profile was terminated at 5 m depth.

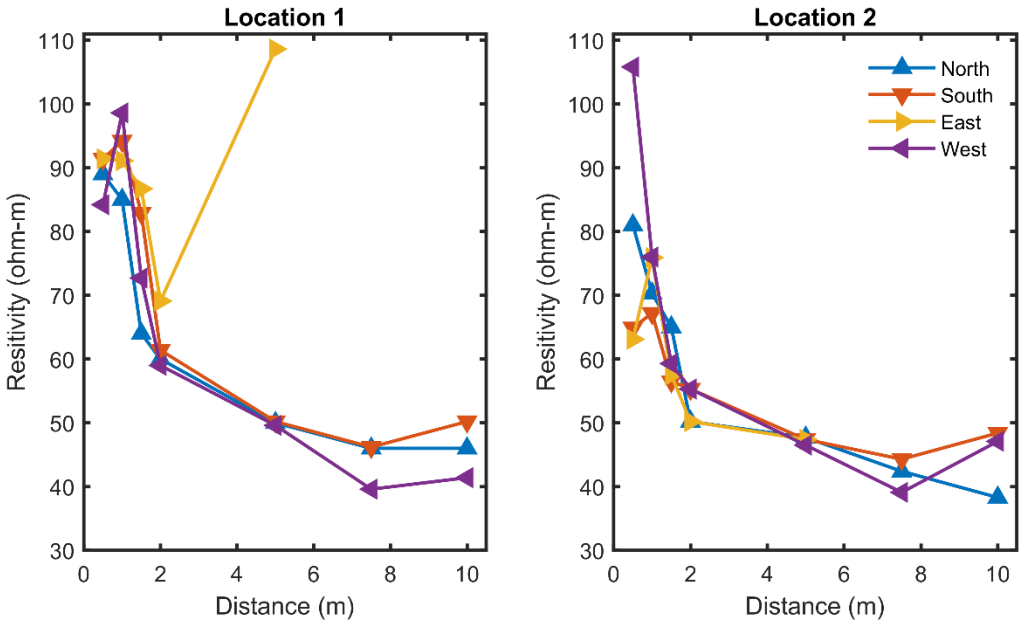

Figure 4. Resistivity survey results from Sanydallah at 2 locations

3.2 Age-depth models

A detailed discussion on the results from the high-resolution chronology can be found in Ramya Bala et al. (2016). Both Core 1 (Figure 5) and Core 2 (Figure 6) show slower accumulation rate in the glacial period followed by higher accumulation rate in the Holocene, evident from the change in slope in the age-depth models. We also observe a jump in radiocarbon ages in Core 1 from ~6100 at 129 cm depth to ~11500 at 133.5 cm depth (Figure 5d). These depths bracket a hiatus in the accumulation.

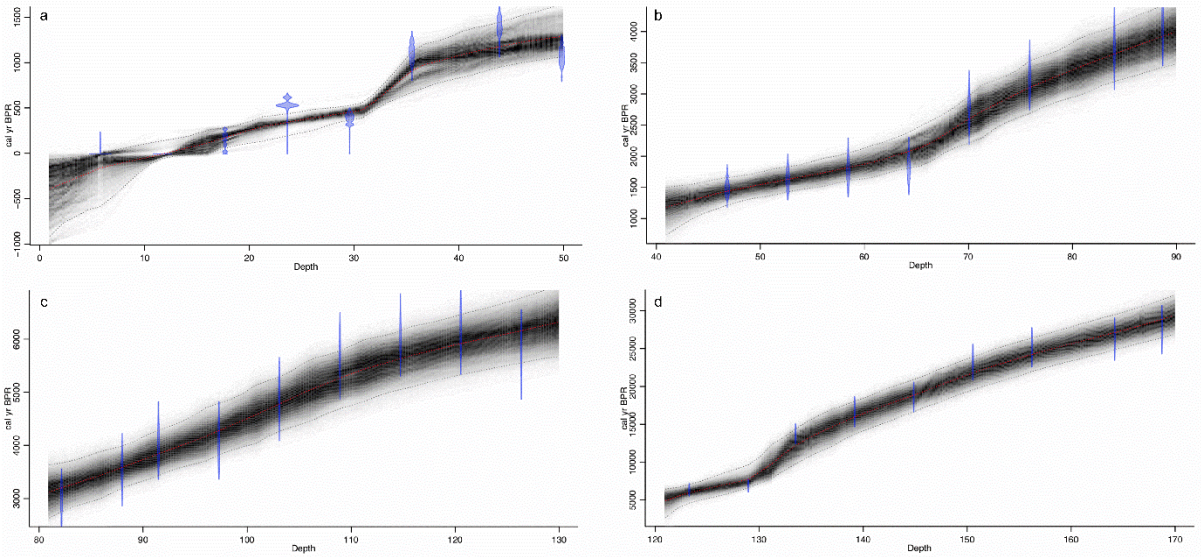

Figure 5: Clockwise from top left – Bayesian Age-depth models for core units 1A, 1B, 1C and 1D, modelled individually to avoid overlapping depths.

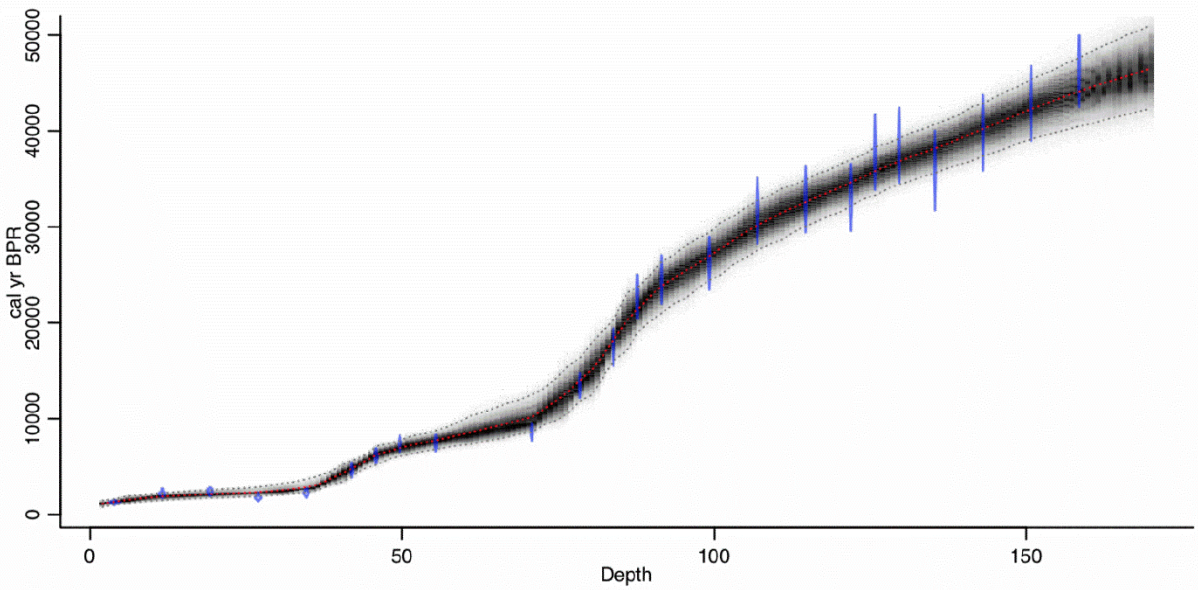

Figure 6: Core 2 modelled as one profile truncated to core unit M above the inversion zone

3.3 Stable Carbon Isotope measurements

Data from $\delta^{13}C$ measurements on cellulose extracts from Cores 1 and 2 are provided in Supplementary Material: Tables 1 and 2 respectively. The values plotted against the median values from Bacon age-depth models are shown in Figure 7. The profile for Core 2 is different from Core 1, indicating different paleovegetation composition, very clear in the glacial period before 10 ka. Also included is data on fires from Kavil et al. (2020) who conducted a study on a pit close to Core 1 (Figure 2). They report two distinct layers of fire using microcharcoal proxies at 22,100 and 3,510 ka. Using alkane derived proxy for surface wetness Paq, they also report two periods of high surface wetness at 4700 and 1320 ka in the valley.

In Core 1, the base of the profile (before the inversion zone) at ~32 ka, shows a C3 vegetation-rich phase. From 25-22 ka, well into the Holocene at ~7500 ka, the C3 vegetation gradually diminishes to give way to C4 dominance. During the Holocene, Core 1 indicates a generally C4 rich vegetation with a short phase of C3 vegetation increase in late-Holocene. In Core 2, we observe a significant glacial-to-interglacial change in mean $\delta^{13}C$ values. The deepest part of the profile from 45 to 20 ka has vegetation which is relatively more C3-rich than the rest of the sequence. From ~20 to 10 ka there is a marked increase in C4 vegetation. In the Holocene, from 10 ka onwards, the profile shows a continual enrichment in C4 vegetation with minor variability until a practically 100% C4 value of ~-11.5‰ in the top ~1000 yrs of the sequence. At some periods – ~15, 4.9 and between 22 and 11.5 ka, the paleovegetation shows a remarkable 100% C4 composition at cellulose values less negative than -12.7‰.

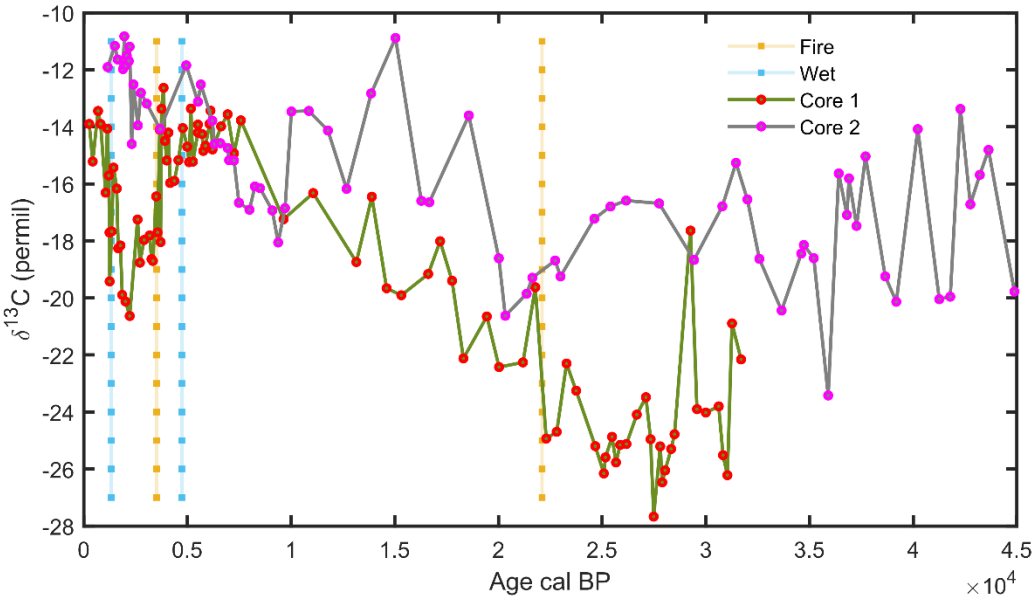

Figure 7: $\delta^{13}C$ results from cellulose extracts, Cores 1 and 2. Fire events (charcoal) and high surface wetness events (alkane derived ratio P_{aq}) from Kavil et al. (2020), study conducted on excavation samples proximate to Core 1.

4. Discussion

We show simultaneously divergent $\delta^{13}C$ values in the last glacial, from ~32 ka to the Holocene, representative of distinctive vegetation states at two adjoining sites within one valley in the montane Nilgiris of the Western Ghats. We also show evidence for an underlying morphological feature beneath Core 1, that makes this site closer to the toe slope, more prone to hydrological disturbances. Why would Cores 1 and 2 that are only ~170m apart in the same valley show such a major difference in past vegetation composition? What would cause such marked changes in vegetation? What role do disturbances such as the fires reported by Kavil et al. (2020) play in maintaining these vegetation states? We explore the various reasons that might have resulted in these patterns indicative of alternative stable vegetation states.

4.1 Differences between Cores 1 and 2

4.1.1 Site characteristics, differences in topography

One significant difference between the two locations is topography. The presence of an apparent toe-slope can be seen from the sudden increase in resistivity in the east direction in location 1. The slight increase in elevation in that direction also prevented us from taking another reading for 10 m depth since the survey can only be done on flat surfaces. While Core 1 shows the presence of a hidden toe-slope, Core 2 is well placed in the middle of the valley away from the boundary.

There is also a difference in hydrology between the two sites. Whereas Core 1 is located to one side of the central channel in Sandynallah; upstream of Core 2 the channel splits into two

creating an island-like microsite, insulating this slightly raised peaty substratum from changes to hydrology. Would these two differences, i.e., the slight elevation and presence of an underground toe slope, or differences in hydrology affect paleo-vegetation dynamics to such an extent? While observations in hydrologic differences are qualitative, we contend that the effects of being proximal to a boundary could explain vegetation differences. Ecotones are known to be more sensitive to small changes in climate whereas greater amplitudes of climatic change are necessary to make an imprint on the paleo-record in the ecological core zone (Caner et al. 2007). And indeed, topography and hydrology might be related to the boundary/edge effects and could constructively interfere to explain the observed changes.

4.1.2 Vegetation differences between Cores 1 and 2

Boundary effects are a pronounced feature within the Alternative Stable States framework. Woody vegetation seem to be growing at opportune sheltered places where the sedgeland meets the sloped grassland. We observe many woody stems close to Core 1 (Figure 1) which is closer to the boundary, whereas Core 2 located in the middle of the valley is not influenced by changes in woody stems. The shola vegetation seems to be occupying this narrow niche in the boundary between sedgeland and grassland. Thus, Core 1 is impacted by boundary dynamics between the sedgeland-shola whereas the vegetation signal recorded in Core 2 is sedgeland throughout.

4.2 Alternative Stable States as a Framework to explain Vegetation Mosaics:

4.2.1 What maintains the sedgeland-shola ecotone?

The ecotone between shola-grassland is pronounced and is maintained by a combination of frost and possibly fires (Ranganathan 1938, Vasanthy 1988, Joshi et al. 2020). What maintains the ecotone between shola-sedgeland? Towards this, we considered the sedgeland-forest dynamics research in Tasmania which has been extremely well-studied in the context of fire-vegetation-sedgeland-grassland-forest dynamics (Bowman and Perry 2017). Fletcher et al (2014) examined sediments in a small patch of non-forest vegetation surrounded by temperate forest. Based on fine-scale pollen, spore, and charcoal analyses of sediments they show that a catastrophic fire drove an irreversible shift from a forested *Cyperaceae–Sphagnum* wetland to a non-forested *Restionaceae* wetland at ca. 7000 ka. Additionally, they show that although the irreversible shift was due to a fire, the new vegetation state gets maintained due to the rhizomatous nature of the colonizing species that creates and promotes water logging, presenting an eco-physical barrier to forest reestablishment. We contend that a similar feedback mechanism is operating at Sandynallah, where waterlogging acts as a barrier to shola sapling establishment.

4.2.2 Applying the alternative stable states paradigm to Sandynallah – a conceptual model

In the montane Nilgiris, the shola-grassland co-occurrence has attracted the attention of ecologists and foresters for nearly a century (Ranganathan 1938; Bor 1938; Meher-Homji 1967). Whereas the grasslands occur on the gentler slopes and ridges, the sholas occupy “sheltered valleys, glens, hollows and depressions” (Ranganathan 1938). In Sandynallah and

other sites that support peat-forming vegetation, a unique niche is created where the sedgeland occupies the valley floor that could have supported shola vegetation. In an alternative stable states framework, the landscape here represents a 3-way stability landscape where a small perturbation is enough for state-change from shola-sedgeland, whereas shola-grassland require a much larger perturbation. As in the conversion observed in Tasmania, the sedge-dominated vegetation and consequent water-logging could create an ecotone for shola-sedgeland, whereas the shola-grassland barrier is underpinned by frost acting as an obstruction for establishment of shola saplings. Our hypothesis is supported by the spatial patterns of shola vegetation in the boundaries of the sedgeland in the raised topography where hydrological differences forced by topography allow for sapling establishment: frost-kill higher in the slopes whereas waterlogging impedes establishment lower down. When ground water is lowered, the boundaries of the sedgeland can become dry, allowing for the waterlogging barrier to be lifted and thus, allowing for the shola saplings to establish themselves. If similar hydrology gets maintained in sustained drier states, the sholas can grow and expand further by a process involving deep-rooting and drying out the surrounding areas, providing a positive feedback to shola establishment. The likelihood that the site can convert from sedgeland to shola is much higher in the case of boundaries as compared to the interior sedgeland due to the elevated topography and presence of deep-rooting shola vegetation that help to dry out the substratum further.

4.3 Interpreting the divergent $\delta^{13}C$ profiles at Sandynallah

4.3.1 Core 1:

Interpreting the results from Core 1 in the light of alternative stable states dynamics, the expectation of arid state is during the glacial period when the summer monsoon is documented to have been weaker (Govil and Divakar Naidu 2011). Starting at the base at ~32 ka, the C3 rich vegetation indicates that the territory around Core 1 could have been in an established shola state at that time due to drier conditions (Figure 7). From 25-22 ka, well into the Holocene at ~7500 ka the shola vegetation gradually diminishes and gives way to sedgeland, which could either indicate a gradually ameliorating hydrology or a disturbance that was damaging to the shola leading to an unstable transition state. The latter interpretation is supported by results from Kavil et al. (2020) who studied sediments from a pit proximate to Core 1 and find charcoal at 22.1 ka. They also present Scanning Electron Microscopy images as evidence that the charcoal has both woody and grass elements (Figure 5 in Kavil et al. (2020)). These results strengthen our claim that shola vegetation existed at that location at 22 ka. It might have been maintained earlier to the fire event due to the drier climate at that time, but the fires might have pushed the system into a transition phase independent of climate, a fundamental characteristic of alternative stable states. The ensuing instability was facilitated by climatic conditions in the last glacial which were not conducive for the immediate re-establishment of sedgeland.

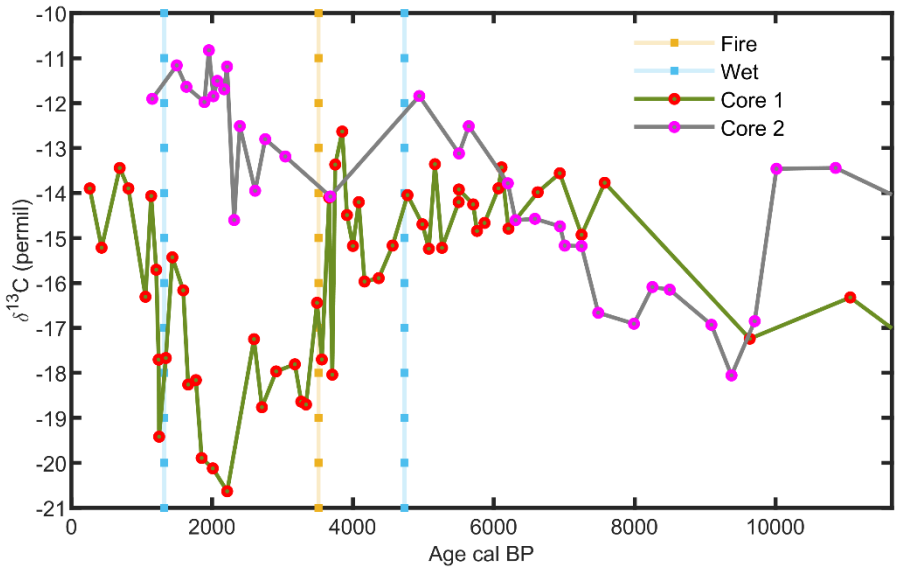

Figure 8. An excerpt from Figure 7 for a closer look at the Holocene

We should also be aware of the hiatus that is observed in Core 1 from ~13 to ~7 ka within a 5 cm difference in depth (See section 3.2.). A similar hiatus is also observed by (Raja et al. 2019) who see a jump in dates from 8 to 16 ka in samples 10 cm apart) at the Parsons valley reservoir nearby. Hence, we do not wish to place emphasis on the samples that have age-depth model dates in this hiatus phase except that it marks the end of the transition phase leading into a complete sedgeland.

From ~7.5 up to ~4 ka, the sedgeland has re-established completely, dominated by C4 vegetation due to wetter conditions. This is supported by a layer of increased surface wetness at 4.7 ka reported by Kavil et al. (2020) through alkane biomarker proxies. From ~4-3.8 ka, C3 vegetation establishment has once again started indicating a gradual change in climate or a disturbance (such as a multi-year drought) that helped the shola establish. Although the mean-state changes, the magnitude is not as large as the sustained shola establishment of the glacial period. Kavil et al. (2020) report a fire layer at ~3.5 ka with charcoal due to the burning of grassy vegetation, which thereby supports the idea that arid conditions prevailed and lead to conditions favourable for a large fire. Since grassy elements burned, the shola vegetation continues to have established itself at the location for a short spell before returning to a sedge-dominated wetland. The return to sedgeland seems to be a result of increased surface wetness, going by the high P_{aq} at 1.32 ka.

4.3.2 Core 2

The location of Core 2 creates two distinct possibilities for what the organic material buried here represents: (a) an autochthonous organic signal from local vegetation, (b) an autochthonous signal overprinted by allochthonous material washed in by the central channel at Sandynallah. The location of Core 2 in a slightly raised substratum, distal from boundary effects, can result in a stable sedgeland state, responding primarily to climate and climatic change. Hence the autochthonous vegetation signal here would be of the sedgeland biomass

growing and accumulating at the site. However, the island-like topography with the central channel forking just ahead of this location might result in deposition of organic material from the slopes and upstream parts of the valley. This allochthonous material would then imprint the signal from the sedgeland state, potentially altering accumulation rates too. Using stable carbon isotopes alone as evidence, we are unable to diagnose the presence of allochthonous deposit of organics at the site. Using supplementary measurements such as grain-size analysis and additional proxies to identify erosional or depositional regimes at the site may help resolve this complexity.

If we follow the possibility of an autochthonous vegetation signal, the $\delta^{13}C$ variations reflect changing C3-C4 species composition in the sedgeland, responding primarily to climate. The disturbances reported by Kavil et al. (2020) seem to show clear impacts on Core 1 through vegetation switches, whereas the effects on vegetation are not apparent in Core 2. We would first like to discuss the change in mean carbon isotopic composition from -17‰ in the last glacial to -14‰ in the interglacial, what climatic factors could lead to a relatively higher C3 biomass in the glacial period, and a very strong C4 signal in the current interglacial?

The factors controlling the relative abundances of C3/C4 plants especially in the last glacial and now in the Holocene are widely debated (Huang 2001; Liu et al. 2005; Schefuß et al. 2005; Sinninghe Damsté et al. 2011). Modelling studies suggest mean annual temperature, atmospheric pCO_2, seasonal water availability (distribution of rainfall in the C3 vs C4 growing seasons) or a combination of these determine relative C3/C4 abundances (Ehleringer and Björkman 1977; Ehleringer 1978; Ehleringer and Pearcy 1983; Winslow et al. 2003). A review of relative C3/C4 abundance since the last glacial to Holocene by Rao et al. (2012) seems to indicate that relative C4 abundance increased (temperature-controlled) in the mid-latitudes, whereas relative C4 abundance decreased in the low-latitudes (precipitation-controlled).

In tropical regimes dominated by seasonal rainfall, changes in paleomonsoon variability are closely tied to vegetation changes. The enrichment in C3 vegetation in the montane grassland-forest belts in the well-studied Mt. Kenya in Africa is closely connected with strengthening monsoons in the Holocene, as is the C4 increase to the arid glacial period (Street-Perrott et al. 2004 and references therein). A similar conclusion using precipitation as a driver of changing C3-C4 composition is drawn by Sukumar et al. (1993) and Rajagopalan et al. (1997) who attribute higher C4 abundance in the last glacial maximum to reduced monsoons, which is also supported by Huang (2001). In montane grassland-forest mosaics where frost acts as a barrier to forest establishment, the significantly lower temperatures in the glacial period could also have resulted in forests retreating and grassland advancing. Whether temperature or precipitation driven, these studies look at C3 tree-C4 grass dynamics at landscape levels. If we look at vegetation dynamics between plants of similar morphology, i.e. C3-C4 sedges and C3-C4 grasses that dominate the sedgeland, what climatic factors could have driven vegetation changes?

C3-C4 altitudinal distribution profiles of grasses of the entire Neotropical Andes are governed by mean annual temperature (Bremond et al. 2012). Their simulations show that the maximum elevation for C4 grasses during the LGM was 2032 m, compared to 2650 m under modern-day

conditions due primarily to temperature differences. The Sandynallah valley occupies a high elevation (~2200 masl) and consequently cool temperatures (modern mean 14º C). This would support a temperature-driven forcing showing relatively C3 enriched vegetation in the last glacial and, subsequently, a warming trend as seen by the C4 enrichment in the Holocene. The positive feedback between waterlogging and rhizomatous vegetation in the middle of the valley floor may have insulated the vegetation from the effects of reduced precipitation. Following the possibility of temperature-forcing, 45 to 20 ka shows the coolest time period in the sequence, from ~20 to 10 ka there is a marked increase in temperatures. In the Holocene, from 10 to 5 ka, the profile shows a consistent increase in C4 vegetation indicative of continual warming. ~5 to 2 ka, the warming eases out and in the 1000 years at the top of the sequence, the temperature is warm enough to support a nearly 100% C4 vegetation.

Apart from temperature, distribution of precipitation in temperate grasslands with distinct growing seasons is an important secondary factor that determines relative C3/C4 abundance (Paruelo and Lauenroth 1996; Murphy and Bowman 2007). While this is yet to be established in tropical montane grasslands, we consider this a very significant factor to be investigated, since Sandynallah receives ~50% of its annual precipitation in the summer and ~30% in the winter. If the C3-C4 abundance in the sedgeland respond to temperatures and seasonality of precipitation in distinct growing seasons, this would need careful further analysis and interpretation.

5. Conclusions

We propose a novel conceptual alternative stable states framework for a tri-stability landscape that includes sedgeland in the well-described shola-grassland mosaics in the Nilgiris. Using this framework, we conclude that the simultaneously diverging stable carbon isotope signatures in Cores 1 and 2 within the Sandynallah valley is evidence for alternative stable states in the past. Core 1 shows shola-sedgeland boundary dynamics with mean vegetation states switching from shola to an unstable phase at 22000 ka due to a fire. This is followed by sedgeland dominance from 7000 ka with a small shift into shola vegetation at 3.75 ka, driven by increasing aridity that eventually results in a large fire (or fires) at 3.5 ka. This phase is followed by a switch to sedgeland dominance again. Core 2 on the other hand shows a stable sedgeland signature and having been insulated from dynamic disturbance-based vegetation state switches, is more likely to preserve responses to changing climate. Our framework with the sedgeland-shola-grassland stable states in the Nilgiris provides us with the necessary lens with which paleovegetation signals here can be reliably interpreted, since vegetation shifts are not always climate-driven in a vegetation mosaic representative of alternative stable states.

Acknowledgements:

PRB would like to thank Rahul Peethambaran for the academic networking, Sandeep Pulla for introduction to the alternative stable states framework and patience with the numerous subsequent clarifications, Jaideep Joshi for support. PRB would also like to thank Prof. Iyue and the team at SBRS, Sandynallah, for permissions and cooperation for sampling. IT would like to acknowledge that this study was partly conducted by the support of Joint Research Grant

for the Environmental Isotope Study of Research Institute for Humanity and Nature, and Japan Society for the Promotion of Science KAKENHI grant number 16H02524. RS was a JC Bose National Fellow (supported by Department of Science and Technology, Government of India) and also Visiting Professor, Institute of Advanced Study, Kyoto University, Japan, during the tenure of this study.

References:

Basu, S., S. Agrawal, P. Sanyal, P. Mahato, S. Kumar, and A. Sarkar. 2015: Carbon isotopic ratios of modern C 3 –C 4 plants from the Gangetic Plain, India and its implications to paleovegetational reconstruction. Palaeogeography, Palaeoclimatology, Palaeoecology 440:22–32.

Behling, H., and V. D. Pillar. 2007: Late Quaternary vegetation, biodiversity and fire dynamics on the southern Brazilian highland and their implication for conservation and management of modern *Araucaria* forest and grassland ecosystems. Philosophical Transactions of the Royal Society B: Biological Sciences 362:243–251.

Blaauw, M., and J. A. Christen. 2011: Flexible Paleoclimate Age-Depth Models Using an Autoregressive Gamma Process. Bayesian Analysis 6:457–474.

Bond, W. J. 2005: Large Parts of the World Are Brown or Black : A Different View on the ' Green World ' Hypothesis Linked references are available on JSTOR for this article : Large parts of the world are World ' hypothesis. 16:261–266.

Bond, W. J., J. A. Silander Jr, J. Ranaivonasy, and J. Ratsirarson. 2008: The antiquity of Madagascar's grasslands and the rise of C $_4$ grassy biomes. Journal of Biogeography 35:1743–1758.

Bor, N. L. 1938: The vegetation of the Nilgiris. Indian Forester 64:601–609.

Bowman, D. M. J. S., and G. L. W. Perry. 2017: Soil or fire: what causes treeless sedgelands in Tasmanian wet forests? Plant and Soil 420:1–18.

Bremond, L., A. Boom, and C. Favier. 2012: Neotropical C3/C4 grass distributions - present, past and future. Global Change Biology 18:2324–2334.

Brenninkmeijer, C. A. M., B. Van Geel, and W. G. Mook. 1982: Variations in the D/H and< sup> 18</sup> O/< sup> 16</sup> O ratios in cellulose extracted from a peat bog core. Earth and Planetary Science Letters 61:283–290.

Caner, L., D. L. Seen, Y. Gunnell, B. R. Ramesh, and G. Bourgeon. 2007: Spatial heterogeneity of land cover response to climatic change in the Nilgiri highlands (Southern India) since the last glacial maximum. The Holocene 17:195–205.

Chaturvedi, R. K., R. Gopalakrishnan, M. Jayaraman, G. Bala, N. V. Joshi, R. Sukumar, and N. H. Ravindranath. 2011: Impact of climate change on Indian forests: a dynamic vegetation modeling approach. Mitigation and Adaptation Strategies for Global Change 16:119–142.

De Vleeschouwer, F., F. M. Chambers, and G. Swindles. 2010: Coring and sub-sampling of peatlands for palaeoenvironmental research. Mires and Peat 7:1–10.

Delcourt, H. R., and P. A. Delcourt. 1997: Pre-Columbian Native American Use of Fire on Southern Appalachian Landscapes. Conservation Biology 11:1010–1014.

Ehleringer, J., and O. Björkman. 1977: Quantum Yields for CO $_2$ Uptake in C $_3$ and C $_4$ Plants: Dependence on Temperature, CO $_2$, and O $_2$ Concentration. Plant Physiology 59:86–90.

Ehleringer, J., and R. W. Pearcy. 1983: Variation in Quantum Yield for CO $_2$ Uptake among C $_3$ and C $_4$ Plants. Plant Physiology 73:555–559.

Ehleringer, J. R. 1978: Implications of quantum yield differences on the distributions of C3 and C4 grasses. Oecologia 31:255–267.

Fletcher, M.-S., S. W. Wood, and S. G. Haberle. 2014: A fire-driven shift from forest to non-forest: evidence for alternative stable states? Ecology 95:2504–2513.

Givelet, N., G. Le Roux, A. Cheburkin, B. Chen, J. Frank, M. E. Goodsite, H. Kempter, M. Krachler, T. Noernberg, N. Rausch, S. Rheinberger, F. Roos-Barraclough, A. Sapkota, C. Scholz, and W. Shotyk. 2004: Suggested protocol for collecting, handling and preparing peat cores and peat samples for physical, chemical, mineralogical and isotopic analyses. Journal of Environmental Monitoring 6:481.

Govil, P., and P. Divakar Naidu. 2011: Variations of Indian monsoon precipitation during the last 32kyr reflected in the surface hydrography of the Western Bay of Bengal. Quaternary Science Reviews 30:3871–3879.

Hirota, M., M. Holmgren, E. H. Van Nes, and M. Scheffer. 2011: Global resilience of tropical forest and savanna to critical transitions. Science 334:232–235.
Hoffmann, W. A., E. L. Geiger, S. G. Gotsch, D. R. Rossatto, L. C. R. Silva, O. L. Lau, M. Haridasan, and A. C. Franco. 2012: Ecological thresholds at the savanna-forest boundary: How plant traits, resources and fire govern the distribution of tropical biomes. Ecology Letters 15:759–768.
Huang, Y. 2001: Climate Change as the Dominant Control on Glacial-Interglacial Variations in C3 and C4 Plant Abundance. Science 293:1647–1651.
Jose, S., A. Sreepathy, B. Mohan Kumar, and V. K. Venugopal. 1994: Structural, floristic and edaphic attributes of the grassland-shola forests of Eravikulam in peninsular India. Forest Ecology and Management 65:279–291.
Joshi, A. A., J. Ratnam, and M. Sankaran. 2020: Frost maintains forests and grasslands as alternate states in a montane tropical forest–grassland mosaic; but alien tree invasion and warming can disrupt this balance. Journal of Ecology 108:122–132.
Jowsey, P. C. 1966: An improved peat sampler. New Phytologist 65:245–248.
Kavil, S. P., P. Ramya Bala, P. Kumar, D. Ghosh, and R. Sukumar. 2020: Climate change and the migration of a pastoralist people c.3500 cal. years BP inferred from palaeofire and lipid biomarker records in the montane Western Ghats, India. BioRxiv:2020.08.15.252189.
von Lengerke, H. J. 1977: The Nilgiris: Weather-Climate of a mountain area in South India. Franz Steiner Verlag, Wiesbaden, p.
Liu, W., Y. Huang, Z. An, S. C. Clemens, L. Li, W. L. Prell, and Y. Ning. 2005: Summer monsoon intensity controls C4/C3 plant abundance during the last 35 ka in the Chinese Loess Plateau: Carbon isotope evidence from bulk organic matter and individual leaf waxes. Palaeogeography, Palaeoclimatology, Palaeoecology 220:243–254.
Meadows, M. E., and H. P. Linder. 1993: Special Paper: A Palaeoecological Perspective on the Origin of Afromontane Grasslands. Journal of Biogeography 20:345.
Meher-Homji, V. M. 1967: Phytogeography of the South Indian Hill Stations. Bulletin of the Torrey Botanical Club 94:230.
Moravek, S., J. Luly, J. Grindrod, and R. Fairfax. 2013: The origin of grassy balds in the Bunya Mountains, southeastern Queensland, Australia. The Holocene 23:305–315.
Murphy, B. P., and D. M. J. S. Bowman. 2007: Seasonal water availability predicts the relative abundance of C_3 and C_4 grasses in Australia. Global Ecology and Biogeography 16:160–169.
Murphy, B. P., and D. M. J. S. Bowman. 2012: What controls the distribution of tropical forest and savanna?: Tropical forest and savanna distribution. Ecology Letters 15:748–758.
Nakamura, T., T. Oda, A. Tanaka, and K. Horiuchi. 2003: High precision 14C age estimation of bottom sediments of Lake Baikal and Lake Hovsgol by AMS. Gekkan Chikyu 42. Tokyo: Kaiyoushuppan.:20–31.
O'Leary, M. H. 1988: Carbon isotopes in photosynthesis. Bioscience:328–336.
Overbeck, G., S. Muller, A. Fidelis, J. Pfadenhauer, V. Pillar, C. Blanco, I. Boldrini, R. Both, and E. Forneck. 2007: Brazil's neglected biome: The South Brazilian Campos. Perspectives in Plant Ecology, Evolution and Systematics 9:101–116.
Paruelo, J. M., and W. K. Lauenroth. 1996: Relative Abundance of Plant Functional Types in Grasslands and Shrublands of North America. Ecological Applications 6:1212–1224.
Pausas, J. G., and W. J. Bond. 2020: Alternative Biome States in Terrestrial Ecosystems. Trends in Plant Science 25:250–263.
Pemadasa, M. A. 1990: Tropical Grasslands of Sri Lanka and India. Journal of Biogeography 17:395.
Pemadasa, M. A., and L. Amarasinghe. 1982: The Ecology of a Montane Grassland in Sri Lanka: I. Quantitative Description of the Vegetation. The Journal of Ecology 70:1.
Raja, P., H. Achyuthan, A. Farooqui, R. Ramesh, P. Kumar, and S. Chopra. 2019: Tropical Rainforest Dynamics and Palaeoclimate Implications since the late Pleistocene, Nilgiris, India. Quaternary Research 91:367–382.

Rajagopalan, G. 1996: Stable isotope paleoclimatology based on tropical peat deposits in Nilgiri hills, southern India.M.S. University of Baroda, Gujarat, India, 117pp.

Rajagopalan, G., R. Sukumar, R. Ramesh, R. K. Pant, and G. Rajagopalan. 1997: Late Quaternary vegetational and climatic changes from tropical peats in southern India - An extended record up to 40,000 years BP. Current Science 73:60–63.

Ramya Bala, P., T. Nakamura, K. Sajeev, and R. Sukumar. 2016: High-resolution age-depth chronology from tropical montane minerotrophic peat in the Sandynallah valley, Western Ghats, southern India: Analytical issues and implications. Quaternary Geochronology 34:12–23.

Ranganathan, C. R. 1938: Studies in the ecology of the shola grassland vegetation of the Nilgiri Plateau. Indian Forester 64.

Rao, Z., F. Chen, X. Zhang, Y. Xu, Q. Xue, and P. Zhang. 2012: Spatial and temporal variations of C3/C4 relative abundance in global terrestrial ecosystem since the Last Glacial and its possible driving mechanisms. Chinese Science Bulletin 57:4024–4035.

Samuel, V. O., M. Santosh, S. Liu, W. Wang, and K. Sajeev. 2014: Neoarchean continental growth through arc magmatism in the Nilgiri Block, southern India. Precambrian Research 245:146–173.

Schefuß, E., S. Schouten, and R. R. Schneider. 2005: Climatic controls on central African hydrology during the past 20,000 years. Nature 437:1003–1006.

Sinninghe Damsté, J. S., D. Verschuren, J. Ossebaar, J. Blokker, R. van Houten, M. T. J. van der Meer, B. Plessen, and S. Schouten. 2011: A 25,000-year record of climate-induced changes in lowland vegetation of eastern equatorial Africa revealed by the stable carbon-isotopic composition of fossil plant leaf waxes. Earth and Planetary Science Letters 302:236–246.

Street-Perrott, F. A., K. J. Ficken, Y. Huang, and G. Eglinton. 2004: Late Quaternary changes in carbon cycling on Mt. Kenya, East Africa: an overview of the δ13C record in lacustrine organic matter. Quaternary Science Reviews 23:861–879.

Stuiver, M., and P. J. Reimer. 1993: Extended 14C data base and revised CALIB 3.0 14C age calibration program. Radiocarbon 35:215–230.

Sukumar, R., H. S. Suresh, and R. Ramesh. 1995: Climate Change and Its Impact on Tropical Montane Ecosystems in Southern India. Journal of Biogeography 22:533.

Sukumar, R., R. Ramesh, R. K. Pant, and G. Rajagopalan. 1993: A delta13C record of late Quaternary climate change from tropical peats in southern India. Letters to Nature 364:703–706.

Suryaprakash, I. 1999: Plant communities in the montane region of Nilgiris, southern India: Analysis of present and past vegetation based on plant-pollen assemblages.pp.

Sutra, J.-P., R. Bonnefille, and M. Fontugne. 1997: Etude palynologique d'un nouveau sondage dans les marais de Sandynallah (massif des Nilgiri, Sud-Ouest de l'Inde). Géographie physique et Quaternaire 51:415–426.

Vasanthy, G. 1988: Pollen analysis of late Quaternary sediments: evolution of upland savanna in Sandynallah (Nilgiris, south India). Review of Palaeobotany and Palynology 55:175–192.

Winslow, J. C., E. R. Hunt, and S. C. Piper. 2003: The influence of seasonal water availability on global C3 versus C4 grassland biomass and its implications for climate change research. Ecological Modelling 163:153–173.

Table 1: Stable carbon isotope results from Core 1

Sample ID	Median Age (cal BP)	Depth (cm)	$\delta^{13}C$ cellulose (‰)
17A	262.9	20.05	-13.9
24A	430.9	28.38	-15.22
28A	687.9	33.14	-13.44
29A	811.2	34.33	-13.9
33A	1053.9	39.1	-16.31
36A	1135	42.67	-14.07
39A	1206.8	46.24	-15.71
41A	1240.4	48.62	-17.71
82B	1247.7	42.16	-19.42
80B	1342.9	44.49	-17.67
78B	1435.5	46.81	-15.43
74B	1589.9	51.47	-16.16
72B	1659.8	53.79	-18.26
69B	1769.6	57.28	-18.16
67B	1851.4	59.6	-19.89
64B	2009.6	63.09	-20.12
61B	2213.8	66.58	-20.63
58B	2594.6	70.07	-17.25
57B	2707.3	71.23	-18.76
55B	2908.7	73.56	-17.97
52B	3175	77.05	-17.81
83C	3266.1	83.33	-18.64
50B	3333.6	79.37	-18.7
86C	3489.4	86.81	-16.44
47B	3557.9	82.86	-17.7
88C	3661.3	89.14	-14.1
45B	3706.2	85.19	-18.04
89C	3748	90.3	-13.37
43B	3847.5	87.51	-12.63
91C	3914.6	92.63	-14.49
92C	3999.2	93.79	-15.18
93C	4082	94.95	-14.2
94C	4163.7	96.12	-15.97
96C	4365.6	98.44	-15.89
98C	4562.2	100.77	-15.17
100C	4774	103.09	-14.05
102C	4985.5	105.42	-14.69
103C	5077.4	106.58	-15.24
104C	5163.7	107.74	-13.36
106C	5264.2	108.91	-15.22
122D	5500.2	122.14	-14.2

108C	5503	112.4	-13.92
111C	5705.9	115.88	-14.25
112C	5760.7	117.05	-14.84
114C	5867.8	119.37	-14.67
118C	6065.1	124.02	-13.9
119C	6109.2	125.19	-13.43
121C	6207.2	127.51	-14.79
125D	6622.8	125.55	-13.98
126D	6935.8	126.68	-13.56
127D	7245.2	127.82	-14.93
129D	7573.1	128.95	-13.77
130D	9632.9	131.23	-17.24
131D	11060.1	132.36	-16.32
133D	13144.4	134.64	-18.74
134D	13890.7	135.77	-16.45
135D	14602.4	136.91	-19.66
136D	15312.4	138.05	-19.91
138D	16608.4	140.32	-19.16
139D	17183.6	141.45	-18.01
140D	17759	142.59	-19.4
141D	18306.1	143.73	-22.12
143D	19436.7	146	-20.65
144D	20025.3	147.14	-22.42
146D	21178.4	149.41	-22.26
147D	21773.7	150.55	-19.62
148D	22300	151.68	-24.93
149D	22805.4	152.82	-24.7
150D	23278.6	153.95	-22.3
151D	23742.1	155.09	-23.25
153D	24664.4	157.36	-25.2
154D	25077.2	158.5	-26.16
163E	25158.3	163.33	-25.59
155D	25473.7	159.64	-24.87
165E	25664.2	165.65	-25.77
156D	25864.6	160.77	-25.15
167E	26167.7	167.98	-25.12
158D	26667.7	163.05	-24.09
171E	27106.6	172.63	-23.48
172E	27333.3	173.79	-24.96
160D	27481.1	165.32	-27.67
174E	27796.7	176.12	-25.2
161D	27895.9	166.45	-26.47
175E	28032.5	177.28	-26.05
162D	28323.9	167.59	-25.3
177E	28486.8	179.6	-24.78

164D	29257.3	169.86	-17.64
182E	29568.3	185.42	-23.9
184E	29995.6	187.74	-24.02
187E	30617.5	191.23	-23.8
188E	30825.1	192.4	-25.52
189E	31037.7	193.56	-26.22
190E	31258	194.72	-20.89
192E	31695.7	197.05	-22.16

Table 2: Stable carbon isotope results from Core 2

Sample ID	Median Age (cal BP)	Depth (cm)	$\delta^{13}C$ cellulose (‰)
01J	1150.3	1.92	-11.91
03J	1497.6	5.77	-11.16
04J	1634.2	7.69	-11.64
06J	1890.7	11.54	-11.98
07J	1954.1	13.46	-10.83
08J	2017.5	15.38	-11.85
09J	2073.4	17.31	-11.51
11J	2170.5	21.15	-11.69
12J	2212	23.08	-11.19
14J	2313.1	26.92	-14.6
15J	2393.3	28.85	-12.51
17J	2610.7	32.69	-13.95
18J	2753.7	34.62	-12.8
19J	3039.3	36.54	-13.19
20J	3678.5	38.46	-14.08
22J	4941.3	42.31	-11.84
02K	5505.1	43.85	-13.12
23J	5643.7	44.23	-12.51
03K	6198.6	45.77	-13.78
24J	6308.2	46.15	-14.6
04K	6583	47.69	-14.57
05K	6938.7	49.62	-14.74
26J	7006.7	50	-15.17
06K	7244.7	51.54	-15.18
07K	7482	53.46	-16.66
09K	7989.3	57.31	-16.91
10K	8251.5	59.23	-16.09
11K	8496.4	61.15	-16.15
13K	9088.8	65	-16.93
14K	9373.7	66.92	-18.06
15K	9703.5	68.85	-16.85
16K	10012.3	70.77	-13.46

17K	10851.4	72.69	-13.44
18K	11772.7	74.62	-14.13
19K	12672	76.54	-16.18
20K	13857.3	78.46	-12.83
21K	15032.6	80.38	-10.88
01L	16275.8	81.92	-16.59
22K	16663.8	82.31	-16.64
23K	18568	84.23	-13.6
03L	20015.8	85.77	-18.61
24K	20325.4	86.15	-20.63
04L	21355.8	87.69	-19.85
25K	21629.5	88.08	-19.29
05L	22729	89.62	-18.69
26K	22987.1	90	-19.25
07L	24618.9	93.46	-17.22
08L	25399.4	95.38	-16.79
09L	26152.4	97.31	-16.58
11L	27743.9	101.15	-16.68
13L	29426.1	105	-18.67
15L	30793	108.85	-16.78
16L	31451.5	110.77	-15.26
17L	31999	112.69	-16.55
18L	32577.9	114.62	-18.63
20L	33649.8	118.46	-20.44
01M	34599	121.92	-18.44
22L	34720.3	122.31	-18.14
02M	35202.5	123.85	-18.6
24L	35897	126.15	-23.42
25L	36405.9	128.08	-15.63
05M	36802.8	129.62	-17.09
26L	36900.2	130	-15.81
06M	37264.4	131.54	-17.47
07M	37698.3	133.46	-15.04
09M	38646.7	137.31	-19.24
10M	39181.2	139.23	-20.14
12M	40217.6	143.08	-14.08
14M	41253.2	146.92	-20.04
15M	41783.8	148.85	-19.96
16M	42274.4	150.77	-13.37
17M	42752.6	152.69	-16.72
18M	43207.9	154.62	-15.68
19M	43628.9	156.54	-14.81
23M	44876.3	162.31	-19.77